Inkjet Printed Nanohydrogel Coated Carbon Nanotubes Electrodes For Matrix Independent Sensing

Supporting Information

Andreas Lesch,[†] Fernando Cortés-Salazar,[†] Véronique Amstutz,[†] Philippe Tacchini[‡] and Hubert H. Girault*[,†]

[†]Laboratoire d'Electrochimie Physique et Analytique, École Polytechnique Fédérale de Lausanne, Station 6, CH-1015 Lausanne, Switzerland

[‡]Edel for Life, PSE-B/EPFL, CH-1015 Lausanne, Switzerland

TABLE OF CONTENTS

SI-1: Reaction scheme of UV photopolymerization
SI-2: Inkjet printing after a too progressed prepolymerization
SI-3: Optimized waveform
SI-4: Inkjet printing of one and two layers of polyacrylamide
SI-5: Wetting test to confirm complete polymerization
SI-6: Substrate dependence of the printing result
SI-7: HR SEM of inkjet printed polyacrylamide
SI-8: Determination of the pore size distribution
SI-9: Height of inkjet printed polyacrylamide
SI-10: Stability of the PA/CNT electrodes
SI-11: Randles-Sevcik analysis
SI-12: Linear sweep voltammetry in diluted orange juice

SI-1 Reaction scheme of UV photopolymerization

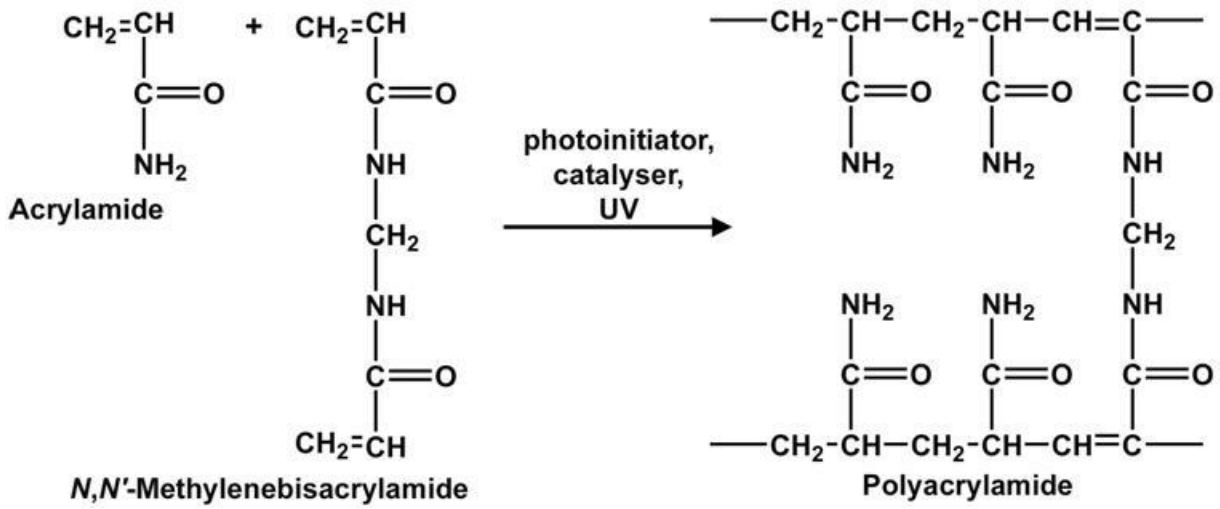

Figure S-1. General reaction scheme of UV photopolymerization of acrylamide and *N,N´*-methylenebis(acrylamide)

The UV photopolymerization of the monomer acrylamide and the cross-linker *N,N´*-methylenebis(acrylamide) to generate the polymer polyacrylamide in aqueous solutions follows a free radical copolymerization reaction mechanism. The reaction is initiated by a radical photoinitiator such as riboflavin. *N,N,N´,N´*-tetramethylethylenediamine (TEMED) is commonly added as a catalyst as it was done in the presented work as well.

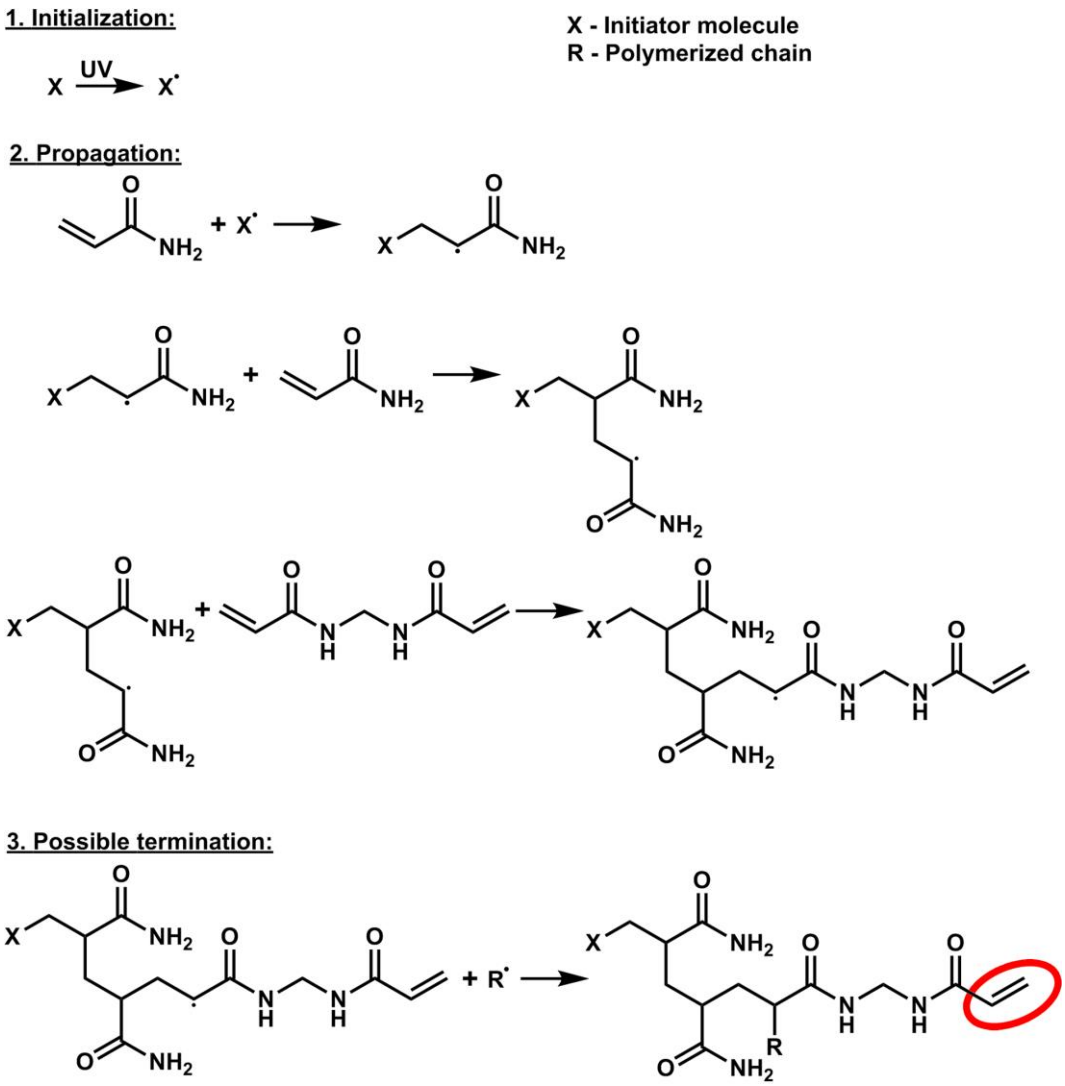

Figure S-2. Possible termination of polymerization in the pre-polymerization process

The initial ink formulation contains the monomer acrylamide and the cross-linker *N*,*N´*-methylenebis(acrylamide). In the free-radical polymerization mechanism acrylamide molecules are added to the radical resulting in chain building and propagation. In case of complete consumption and degradation of radicals and radical sources, the polymerization reaction is aborted. Herein, it is assumed that free vinylic groups (marked by a red ellipse) from the added *N*,*N´*-methylenebis(acrylamide) could provide the radical sources for reinitialization in the inkjet printing process after prepolymerization.

SI-2 Inkjet printing after a too progressed prepolymerization

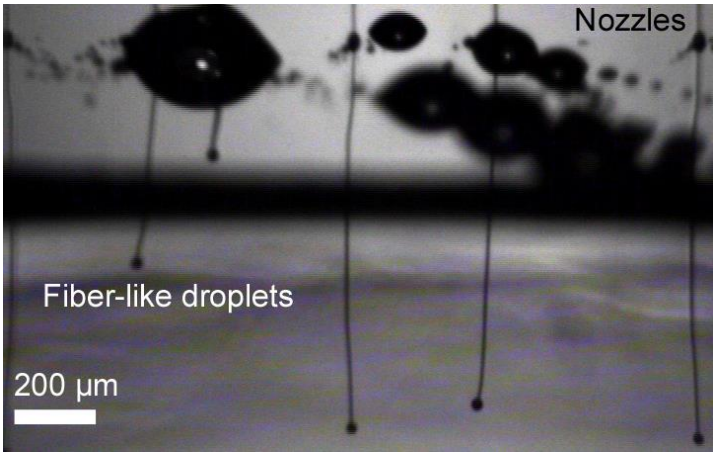

Figure S-3. Fiber-like droplet formation during printing with a prepolymerized ink of a viscosity higher than 2 mPa·s. Picture taken with the drop view camera of the used Dimatix DMP 2831 printer.

The prepolymerization process is critical in terms of the applied conditions such as the concentration of monomer, cross-linker, catalyst and photoinitiator, the UV intensity and the stirring rate of the solution. In case the polymerization and cross-linking is too much progressed, macromolecular structures of PA are obtained that avoid proper jetting by a possible blocking of the nozzles or the formation of fiber-like droplets. The latter are jetted without control and their reproducibility is as shown in Figure S-3. In this particular case a viscosity higher than 2 mPa·s has been achieved due to a higher concentration of catalyst and photoinitiator than the optimum amount.

SI-3 Optimized waveform

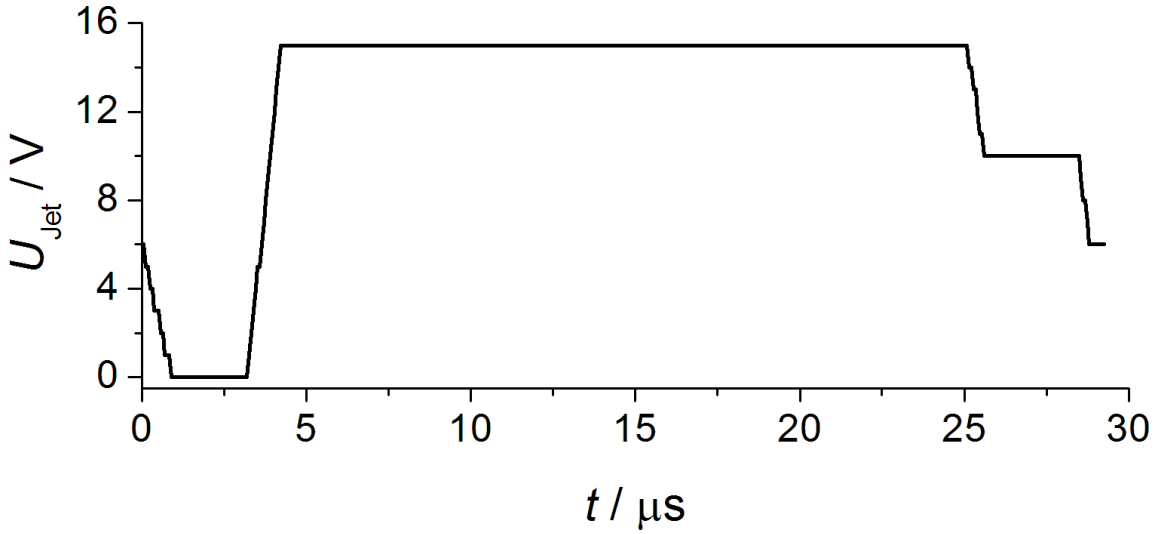

Figure S-4. Applied waveform to the piezo-driven printhead for jetting of the acrylamide/bis ink by using the 10 pL cartridges of the Dimatix DMP-2831 printer.

SI-4 Inkjet printing of one and two layers of polyacrylamide

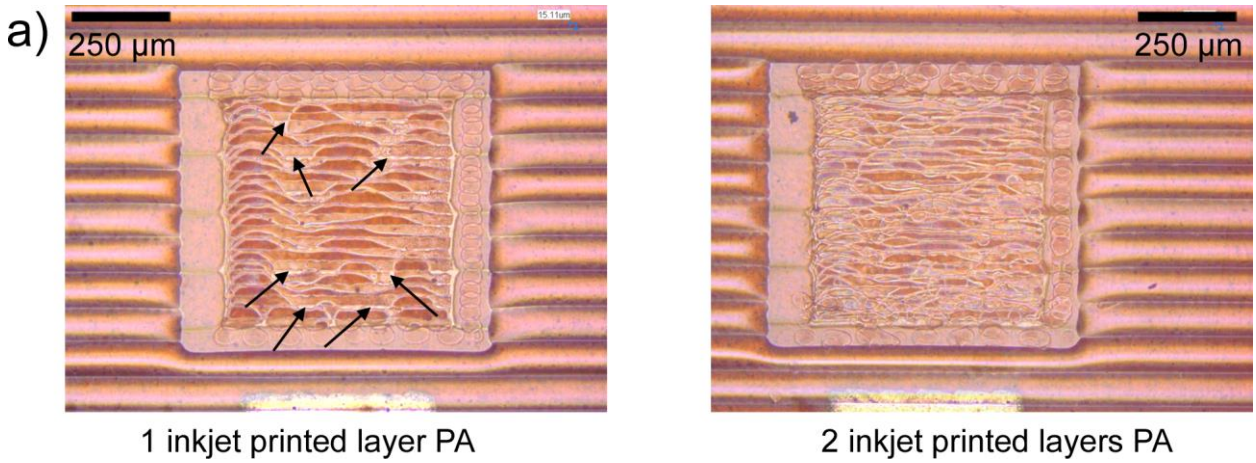

Figure S-5. Laser scanning micrographs of inkjet-printed PA on CNT electrodes. a) 1 inkjet-printed layer of PA. b) 2 inkjet-printed layers PA.

Inkjet printing of 1 layer of PA resulted in a PA layer with some uncovered areas that can easily be identified in the pattern (arrows in Figure S-5a indicate exemplary areas). Printing a second layer of PA using the same printing parameters covered the CNT electrode completely (Figure S-5b). Experimental details are given in the main manuscript.

SI-5 Wetting test to confirm complete polymerization

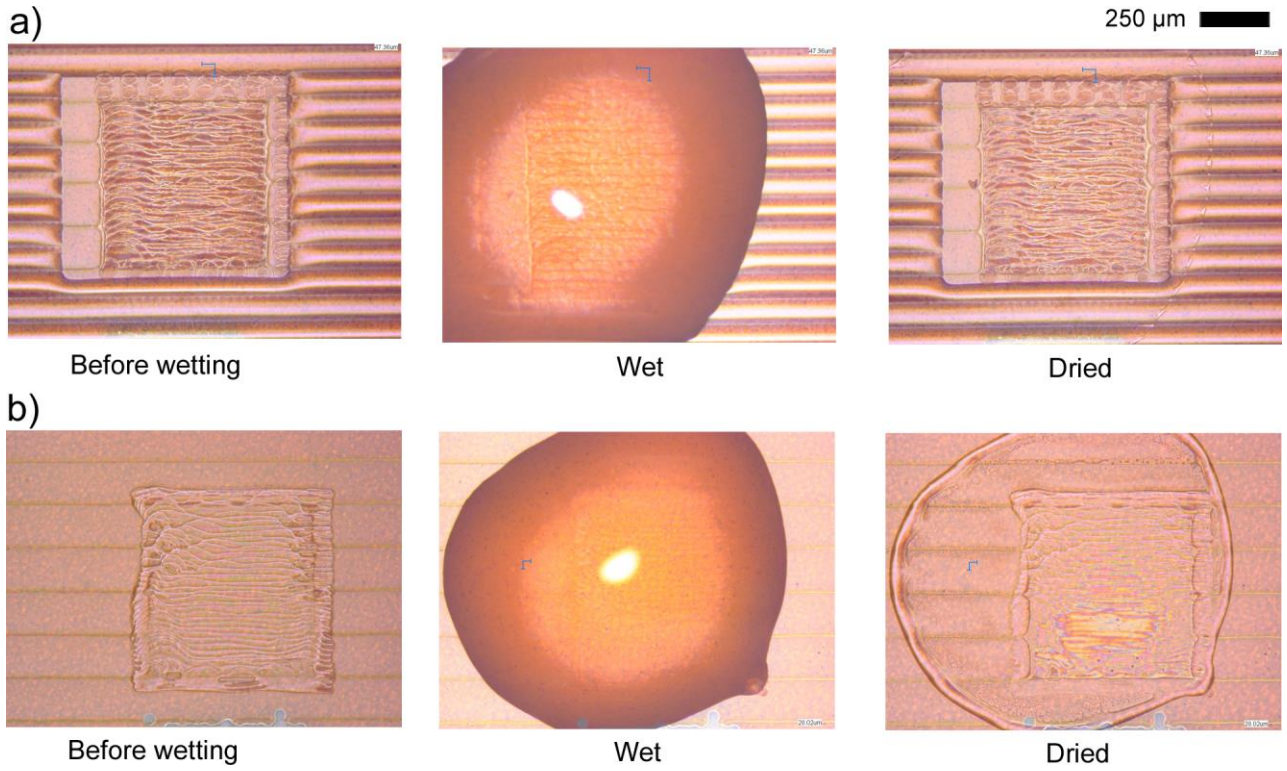

Figure S-6. Wetting test of inkjet-printed PA/CNT electrodes using a) the prepolymerization concept and b) ink composition B (see below). A 0.5 μL droplet of H_2O was dropped on the gel electrodes and dried at air.

Washing the printed pattern with DI water is one important experiment to confirm the successful polymerization of the acrylamide/bis ink, i.e., the existence of a PA film as well as its stable link to the CNT substrate. Not polymerized material will easily be washed away. We have dropped 0.5 μL of DI water on the printed structure and let it dry at air. Using the optimized printing parameters (printing details in the main manuscript) led to a completely polymerized and stable film (Figure S-6a).
Alternatively, using an ink composition with added PA macromolecules (Table S-1) in order to increase the viscosity up to 1.8 mPa·s without prepolymerization did not result in a stable and completely polymerized layer (Figure S-6b). The same printing parameters have been used as for the optimized ink. The obtained film was essentially removed by the DI water.

Table S-1: Ink composition with PA macromolecules:
- 14.9% (w/v) acrylamide/bis (2.6% C)
- 3.1% (w/v) polyacrylamide (average MW 10'000 g mol^{-1})
- 5 μg/mL Riboflavin (photoinitiator)
- 0.11% (w/v) TEMED (catalyst)
- 0.68 μL/mL Triton-X 100 (surfactant)
- viscosity 1.8 mPa·s

SI-6 Substrate dependence of the printing result

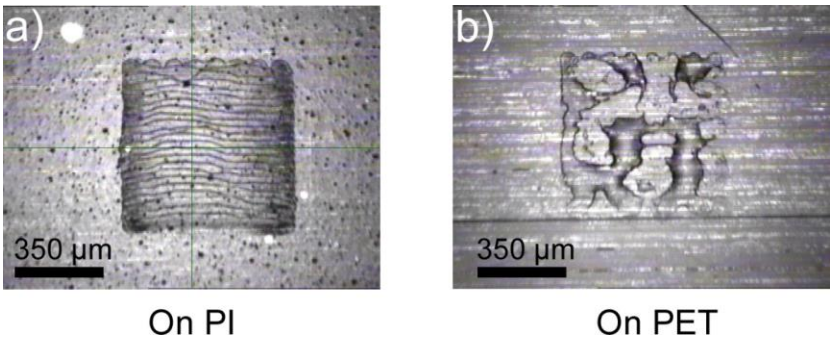

Figure S-7. Substrate dependence of the inkjet printing and UV photopolymerization of acrylamide/bis ink. View on a) PI and b) PET substrates using the fiducial camera of the Dimatix DMP-2831 printer. The same printing parameters have been applied for both samples using the same ink.

We obtained that the selection of the right substrate is crucial for the simultaneous IJP and UV photopolymerization of the acrylamide/bis containing ink. On polyimide (PI) a well defined pattern of PA is achieved (Figure S-7a) whereas on poly(ethylene terephthalate) (PET) no polymerization could be obtained simultaneously to printing (Figure S-7b). Indeed, it has been reported that PET is photodegraded by UV irradiation to form carboxyl groups especially at the outermost layer of the exposed film (G.J.M Fechine, M.S. Rabello, R.M. Souto Maior, L.H. Catalani; Surface characterization of photodegraded PET. The effect of ultraviolet absorbers; *Polymer* **2004**, *45*, 2303-2308). Therefore, upon the UV photopolymerization step, the PET surface might undergo surface and structural changes that modify the ink-substrate interaction into a non-optimized condition. Moreover, thermal effects coming from the use of a mercury UV lamp for the photopolymerization process cannot be neglected. Therefore, bare PI and CNT/PI surfaces represent favorable substrates for the presented IJP concept of PA films. In the main manuscript, the polymerization has been carried out on stand-alone CNT electrodes which have shown a similar polymerization result compared to the bare PI surface. The optimized printing parameters, as given in the main manuscript, were applied.

SI-7 HR SEM of inkjet printed polyacrylamide

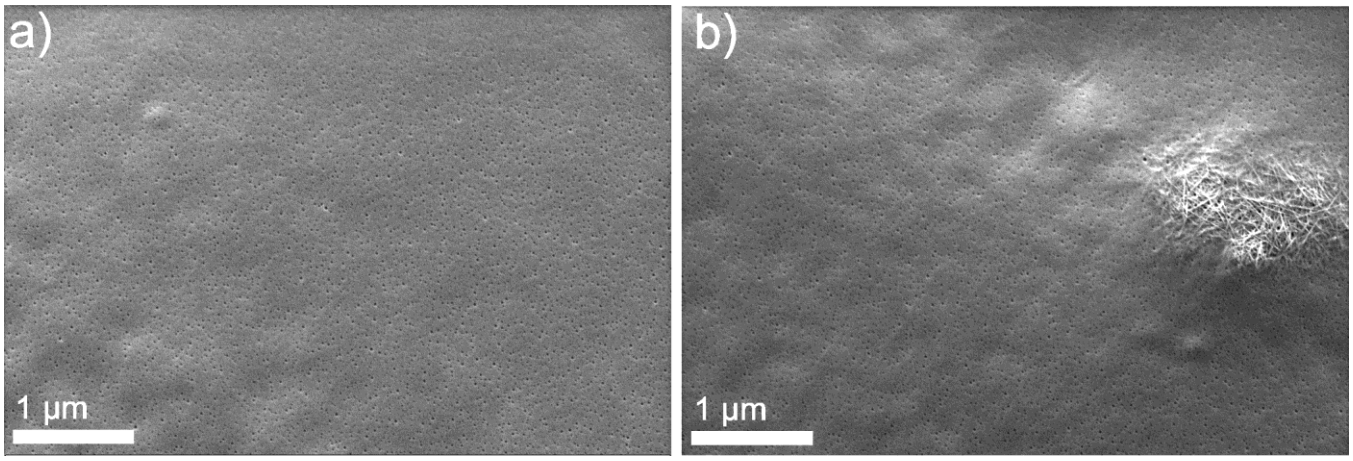

Figure S-8. a) HR SEM of defect-free PA/CNT electrodes. b) Sample with a defect in the PA layer.

The HR SEM of a compact PA layer shows well distributed nanopores (Figure S-8a). A pattern with a defect in the PA layer demonstrates the small thickness of the PA layer in the center of a printed line within a complete PA/CNT electrode (Figure S-8b).

SI-8 Determination of the pore size distribution

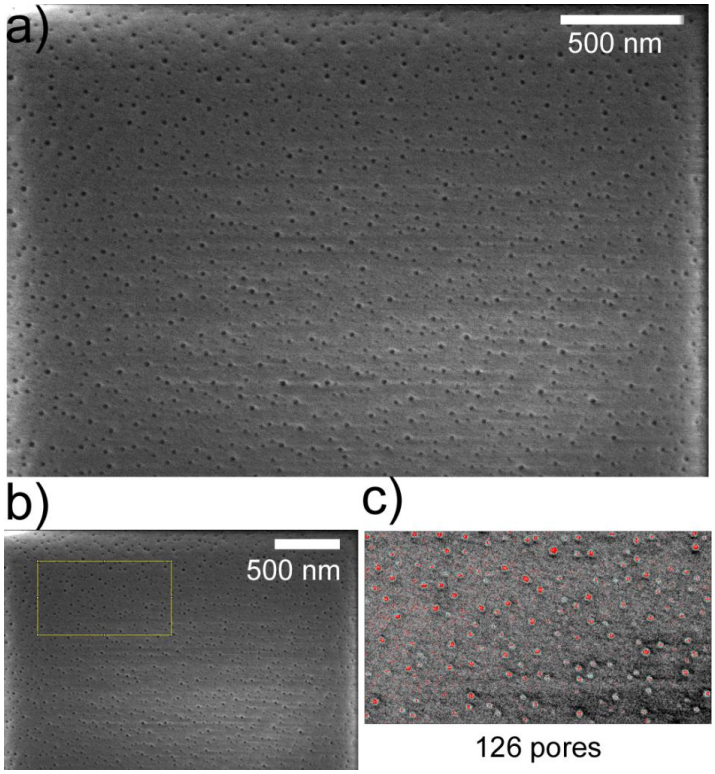

Figure S-9. Determination of the pore size distribution using ImageJ software. a) HR SEM picture of 2 IJPL PA on 4 IJPL CNT electrodes. b) Yellow rectangle illustrates selected area for pore size analysis. c) 126 pores were found by the ImageJ software for the analysis.

The average size of the nanopores was determined by applying ImageJ software to a representative HR SEM of a freeze dried inkjet printed PA sample. 126 well distributed nanopores were identified within an area of 0.58 μm^2 in the hydrogel layer with an average diameter of (13.3 ± 9.1) nm (Figure S-9). The estimated pore density is 216 pores μm^{-2}.

SI-9 Height of inkjet printed polyacrylamide

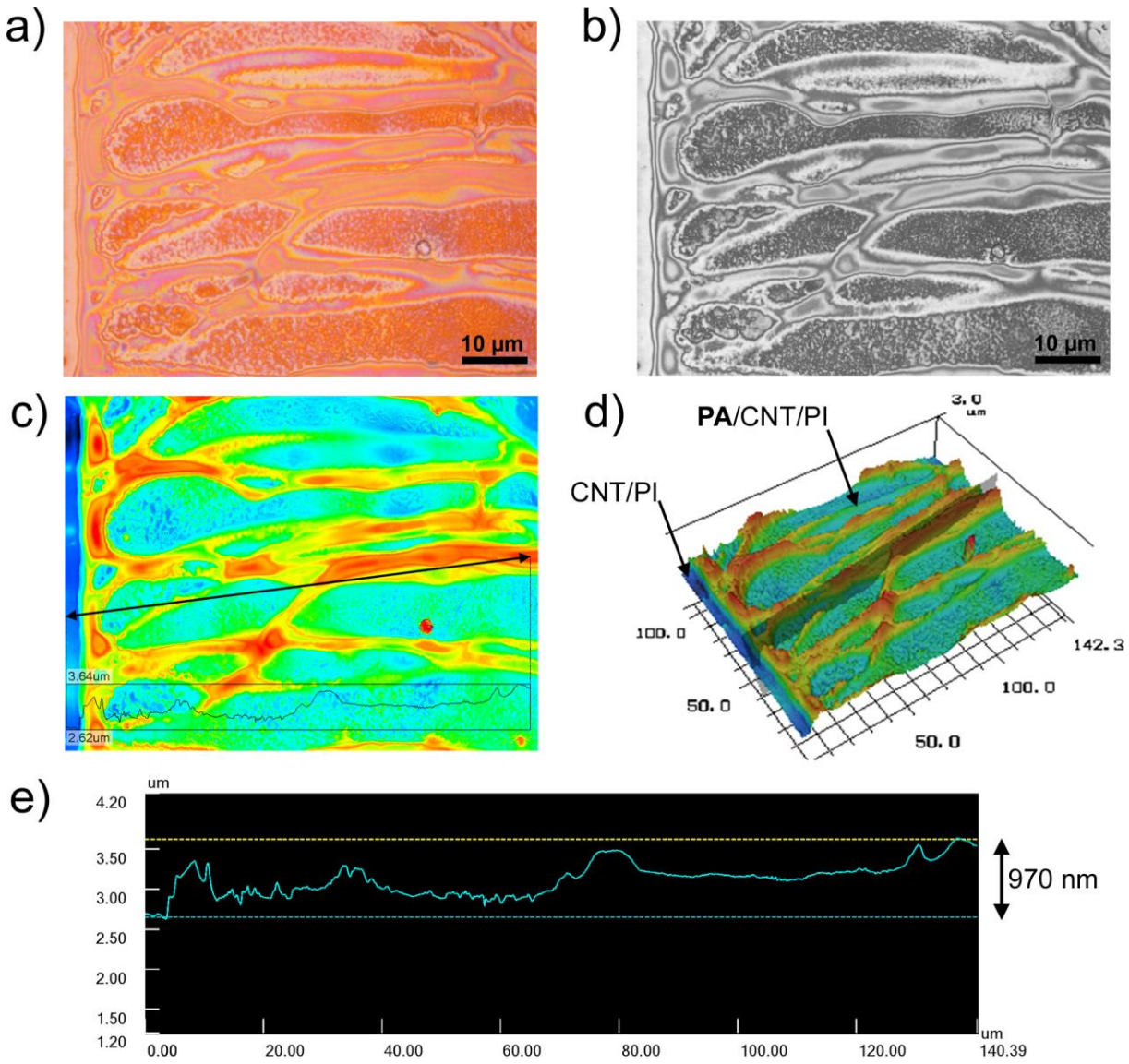

Figure S-10. Topography of inkjet printed PA on a CNT/PI surface measured with a laser scanning microscope. a) Optical micrograph. b) Laser scanning micrograph. Topography image as c) 2D plot and d) 3D plot with location of selected e) height profile.

The topography of the inkjet printed PA layer was investigated using laser scanning microscopy. Due to the coffee ring effect the rim of a printed line was thicker than the center. Therefore, the determined thickness of the PA film ranged from around 50 nm in the middle of a printed line up to 1000 nm at its rim.

SI-10 Stability of the PA/CNT electrodes

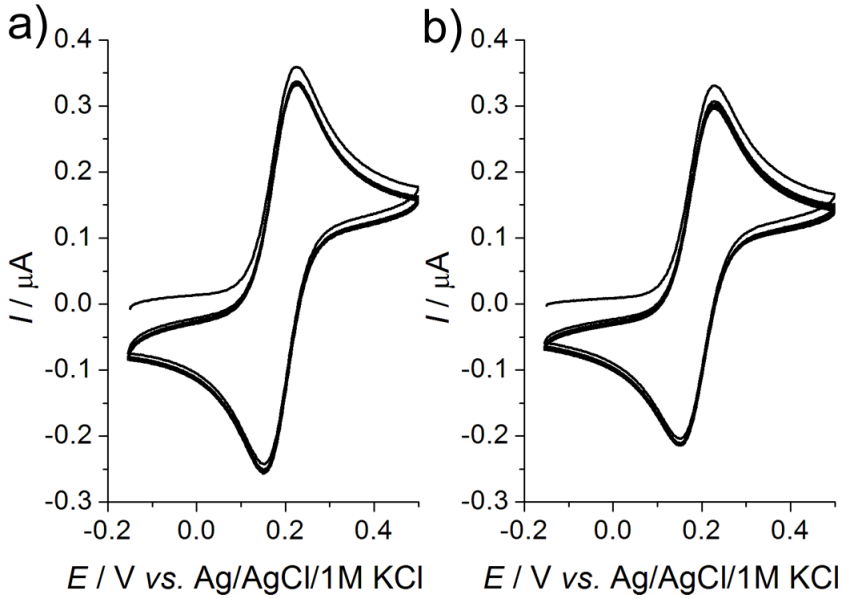

Figure S-11. Stability of the a) bare CNT and b) PA/CNT electrodes during CV in 0.5 mM FcMeOH and 0.1 M KCl with ν = 100 mV·s^{-1} and number of cycles = 21.

In order to demonstrate the functionality and stability of the PA hydrogel/CNT electrodes CVs of 21 cycles were performed in FcMeOH solution. The electrodes were used directly after printing and washing without any further treatment. Indeed, the recorded signals were as stable as for pure CNT electrodes. These results show that the hydrogel layer can be applied without pretreatment such as wetting and that the response is stable over time.

SI-11 Randles-Sevcik analysis

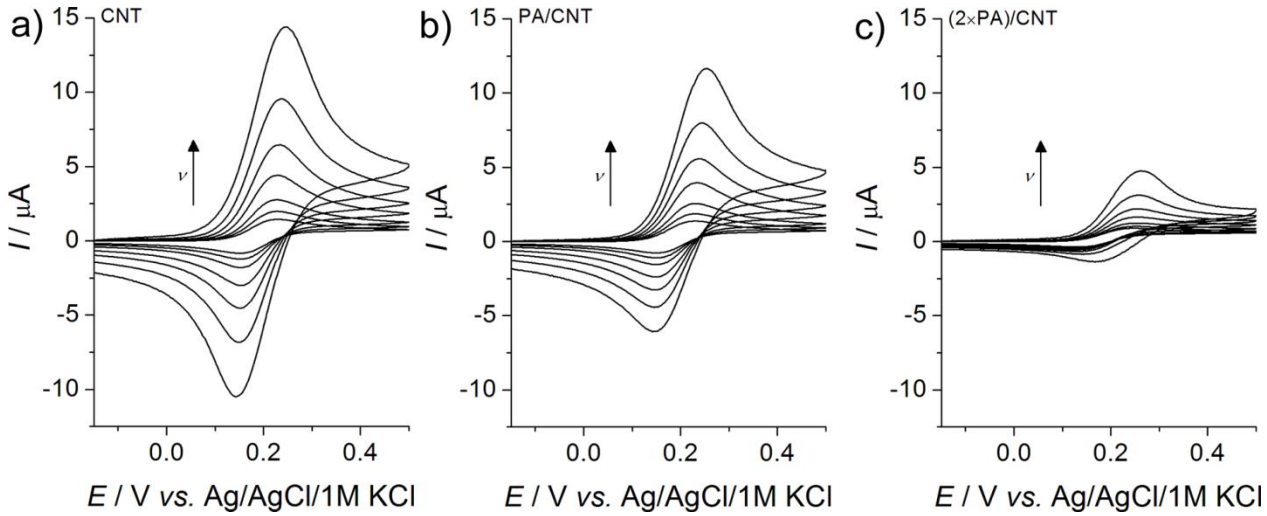

Figure S-12. Scan rate dependence of a) bare CNT, b) PA/CNT and c) (2×PA)/CNT electrodes in 4 mM FcMeOH and 0.1 M KCl. Various *v* in mV·s^{-1}: 25, 50, 100, 250, 500, 1000 and 2000.

The Randles-Sevcik equation is as follows,

$$I_{\mathrm{pa}} = 0.4463 \cdot \left(\frac{F^3}{RT}\right)^{\frac{1}{2}} \cdot n^{\frac{3}{2}} \cdot A_{\mathrm{m}} \cdot D^{\frac{1}{2}} \cdot c^* \cdot v^{\frac{1}{2}}$$

The Randles-Sevcik equation at room temperature can be written as:

$$I_{\mathrm{pa}} = 2.69 \cdot 10^5 \cdot n^{\frac{3}{2}} \cdot A_{\mathrm{m}} \cdot D^{\frac{1}{2}} \cdot c^* \cdot v^{\frac{1}{2}}$$

A_{m} – microscopic electrode area in cm^2. In the main manuscript $A_{\mathrm{m}} = A_{\mathrm{g}}$.

I_{pa} – anodic peak current in A.

n – number of transferred electrons.

D – diffusion coefficient of the redox mediator in cm^2·s^{-1}.

v – scan rate in V·s^{-1}.

c^* – concentration of the redox mediator in bulk solution in mol·cm^{-3}.

SI-12 Linear sweep voltammetry in diluted orange juice

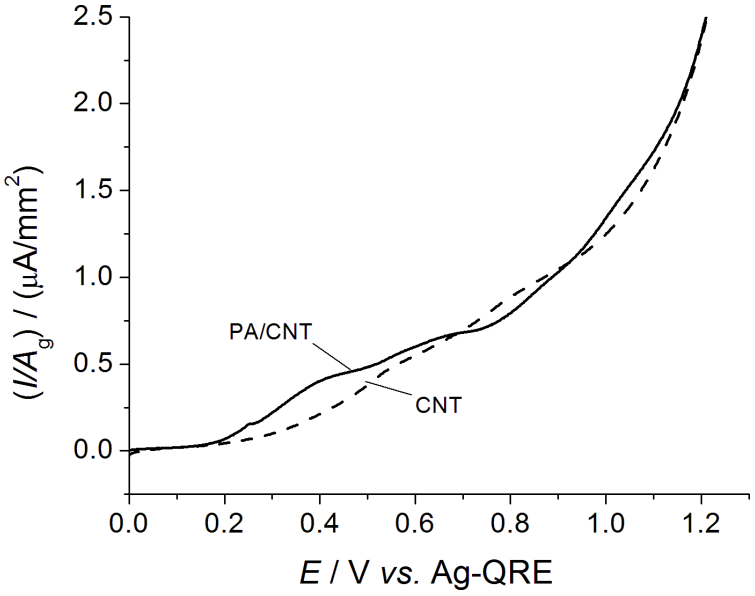

Figure S-13. LSVs of PA/CNT (solid line) and CNT (dashed line) electrodes in filtered orange juice 10 fold diluted in 0.1 M acetate buffer (pH 3.8). Scan rate ν = 100 mV·s^{-1}.

The matrix effect could also be overcome diluting 10 fold the filtered orange juice sample (Figure S-13).